
Back2Future: Leveraging Backfill Dynamics for Improving Real-time Predictions in Future

Harshavardhan Kamarthi, Alexander Rodríguez, B. Aditya Prakash
College of Computing
Georgia Institute of Technology
{harsha.pk, arodriguez, badityap}@gatech.edu

Abstract

In real-time forecasting in public health, data collection is a non-trivial and demanding task. Often after initially released, it undergoes several revisions later (maybe due to human or technical constraints) - as a result, it may take weeks until the data reaches to a stable value. This so-called 'backfill' phenomenon and its effect on model performance has been barely studied in the prior literature. In this paper, we introduce the multi-variate backfill problem using COVID-19 as the motivating example. We construct a detailed dataset composed of relevant signals over the past year of the pandemic. We then systematically characterize several patterns in backfill dynamics and leverage our observations for formulating a novel problem and neural framework Back2Future that aims to refine a given model's predictions in real-time. Our extensive experiments demonstrate that our method refines the performance of top models for COVID-19 forecasting, in contrast to non-trivial baselines, yielding 18% improvement over baselines, enabling us obtain a new SOTA performance. In addition, we show that our model improves model evaluation too; hence policy-makers can better understand the true accuracy of forecasting models in real-time.

1 Introduction

The current COVID-19 pandemic has challenged our response capabilities to a large disruptive event, affecting the health and economy of millions of people. A major tool in our response has been forecasting epidemic trajectories, which has provided lead time to policy makers to optimize and plan interventions [21]. Broadly two classes of approaches have been devised: traditional mechanistic epidemiological models [40, 48], and the fairly newer statistical approaches [5, 1, 31] including deep learning models [1, 17, 33, 38], which have become among the top performing ones for multiple forecasting tasks [37]. These also leverage newer digital indicators like search queries [19, 45] and social media [16, 26]. As noted in multiple previous works [29, 4], epidemic forecasting is a challenging enterprise because it is affected by weather, mobility, strains, and others.

However, *real-time* forecasting also brings new challenges. As noted in multiple CDC real-time forecasting initiatives for diseases like flu [30] and COVID-19 [14], there are concerns with respect to the initial releases of data. Typical public health data is revised many a times after its initial release (known as the 'backfill' phenomenon), which, from our analysis, it may need up to 21 weeks to reach to its final stable value. The various factors that effect backfill are multiple and complex, ranging from surveillance resources to human factors like coordination between health institutes and government organization within and across regions [9, 37, 2].

While previous works have addressed anomalies [27], missing data [46], and data delays [49] in general time-series problems, the backfill problem has not been addressed. In contrast, the topic of revisions has not received as much attention, with few exceptions. For example in epidemic

forecasting, a few papers have either (a) mentioned about the ‘backfill problem’ and its effects on performance [9, 39, 2, 36] and evaluation [37]; or (b) proposed to address the problem via simple models like linear regression [8] or ‘backcasting’ [5] the observed targets. However they focus only on revisions in the *target*, and study only in context of influenza forecasting, which is substantially less noisy and more regular than the novel COVID-19 pandemic. In economics, [12] surveys several domain-specific [6] or essentially linear techniques for data revision/correction behavior of the source of several macroeconomic indicators [15], e.g. job unemployment numbers.

Motivated from above, we study the more challenging problem of multi-variate backfill for both features and targets. We go further beyond prior work and also show how to leverage our insights for a more general neural framework to *improve* both model predictions (i.e. *refinement* of the modeler’s perspective) and model performance evaluation (i.e. *rectification* from the evaluator’s perspective). Our specific contributions are the following:

- **Multi-variate backfill problem:** We introduce the multi-variate backfill problem using real-time epidemiological forecasting as the motivating example. In this challenging setting, which generalizes (the limited) prior work, the forecast targets as well as exogenous features are subject to retrospective revision. Using a carefully collected diverse dataset for COVID-19 forecasting for the past year, we discover several patterns in backfill dynamics, show that there is a significant difference in real-time and revised feature measurements and highlight the negative effects of using unrevised features for incidence forecasting in different models both for model performance and evaluation. Building on our empirical observations, we formulate the problem BFRP, which aims to ‘correct’ given model predictions to achieve better performance on eventual fully revised data.

- **Spatial and Feature level backfill modelling to refine model predictions:** Motivated by the patterns in revision and observations from our empirical study, we propose a deep-learning model Back2Future (B2F) to model backfill revision patterns and derive latent encodings for features. In contrast to [24] who deal with multiple sequences of labels using attention to combines large number of features spanning across multiple regions, B2F combines Graph Convolutional Networks that capture sparse, cross-feature and cross-regional backfill dynamics similarity and deep sequential models that capture temporal dynamics of each features’ backfill dynamics across time. The latent representation of all features is used along with history of model’s predictions to improve different classes of models trained on real-time targets, to predict targets closer to revised ground truth values. Our technique can be used as a ‘wrapper’ to improve model performance of any forecasting model (mechanistic/statistical).

- **SOTA performance and improved model evaluation:** We perform extensive empirical evaluation to show that Back2Future consistently improves performance of different classes of top performing COVID-19 forecasting models (from the CDC COVID-19 Forecast Hub, including the top-performing official ensemble) significantly and as a direct consequence, provide a new state-of-the-art model – B2F-refined Covid Hub Ensemble – for the (real-time) COVID-19 forecasting task. We also utilize B2F to help forecast evaluators and policy-makers better evaluate the ‘eventual’ true accuracy of participating models (against revised ground truth, which may not be available until weeks later). This allows the model evaluators to more quickly estimate models that perform better w.r.t revised stable targets instead of potentially misleading current targets. Our methodology can be adapted for other time-series forecasting problems in general.

2 Nature of backfill dynamics

In this section, we study important properties of the revision dynamics of our signals. We introduce some concepts and definitions to aid in understanding of our empirical observations and method.

Real-time forecasting. We are given a set of signals $\mathcal{F} = \text{Reg} \times \text{Feat}$, where set Reg is the set of all regions (where we want to forecast) and set Feat contains our features and forecasting target(s) for each region. At prediction week t , $x_{i,1:t}^{(t)}$ is a time series from 1 to t for feature i , and the set of all signals results in the multi-variate time series $\mathcal{X}_{1:t}^{(t)}$ ¹. Similarly, $\mathcal{Y}_{1:t}^{(t)}$ is the forecasting target(s) time series. Further, let’s call all data available at time t , $\mathcal{D}_{1:t}^{(t)} = \{\mathcal{X}_{1:t}^{(t)}, \mathcal{Y}_{1:t}^{(t)}\}$ as *real-time sequence*. For clarity we refer to ‘signal’ $i \in \mathcal{F}$ as a sequence of either a feature or a target, and denote it as $d_{i,1:t}^{(t)}$.

¹In practice, delays are possible too, i.e, at week t , we have data for some feature i only until $t - \delta_i$. All our results incorporate these situations. We defer the minor needed notational extensions to supplement for clarity.

Thus, at prediction week t , the real-time forecasting problem is: *Given $\mathcal{D}_{1:t}^{(t)}$, predict next k values of forecasting target(s), i.e. $\hat{y}_{t+1:t+k}$.* Typically for CDC settings and this paper, our time unit is week, $k = 4$ (up to 4 weeks ahead) and our target is COVID-19 mortality incidence (Deaths).

Revisions. Data revisions (‘backfill’) are common. At prediction week $t + 1$, the real-time sequence $\mathcal{D}_{1:t+1}^{(t+1)}$ is available. In addition to the length of the sequences increasing by one (new data point), values of $\mathcal{D}_{1:t+1}^{(t+1)}$ already in $\mathcal{D}_{1:t}^{(t)}$ may be revised i.e., $\mathcal{D}_{1:t}^{(t)} \neq \mathcal{D}_{1:t}^{(t+1)}$. Note that previous work has studied backfill limited to $\mathcal{Y}^{(t)}$, while we address it in both $\mathcal{X}^{(t)}$ and $\mathcal{Y}^{(t)}$. Also note that the data in backfill is the same used for real-time forecasting, but just seen from a different perspective.

Backfill sequences: Another useful way we propose to look at backfill is by focusing on revisions of a single value. Let’s focus on value of signal i at an *observation week* t' . For this observation week, the value of the signal can be revised at any $t > t'$, which induces a sequence of revisions. We refer to *revision week* $r \geq 0$ as the relative amount of time that has passed since the observation week t' .

Defn. 1. (Backfill Sequence BSEQ) For signal i and observation week t' , its backfill sequence is $\text{BSEQ}(i, t') = \langle d_{i,t'}^{(t')}, d_{i,t'}^{(t'+1)}, \dots, d_{i,t'}^{(\infty)} \rangle$, where $d_{i,t'}^{(t')}$ is the initial value of the signal and $d_{i,t'}^{(\infty)}$ is the final/stable value of the signal.

Defn. 2. (Backfill Error BERR) For revision week r of a backfill sequence, the backfill error is $\text{BERR}(r, i, t') = |d_{i,t'}^{(t'+r)} - d_{i,t'}^{(\infty)}| / |d_{i,t'}^{(\infty)}|$.

Defn. 3. (Stability time STIME) of a backfill sequence BSEQ is the revision week r^* that is the minimum r for which the backfill error $\text{BERR} < \epsilon$ for all $r > r^*$, i.e., the time when BSEQ stabilizes.

Note: We ensured that BSEQ length is at least 7, and found that in our dataset most signals stabilize before $r = 20$. For $d_{i,t'}^{(\infty)}$, we use $d_{i,t'}^{(t_f)}$, at the final week t_f in our revisions dataset. In case we do not find $\text{BERR} < \epsilon$ in any BSEQ, we set STIME to the length of that BSEQ. We use $\epsilon = 0.05$.

2.1 Dataset description

We collected important publicly available signals from a variety of trusted sources that are relevant to COVID-19 forecasting to form the COVID-19 *Surveillance Dataset* (CoVDS). See Table 1 for our 20 features (hence $|\text{Feat}| = 21$, including Deaths). Our revisions dataset contains signals that we collected every week since April 2020, and ends on February 2021. Our analysis covers 30 observation weeks from mid-May 2020 to mid-December 2020 (to ensure all our backfill sequences are of length at least 7) for all $|\text{Reg}| = 50$ US states.

Patient line-list: are traditional surveillance signals used in epidemiological models [34, 8, 5] derived from line-list records e.g. hospitalizations from CDC [7], positive cases, ICU admissions etc from COVID Tracking [13]. **Testing:** measure changes in testing also from CDC and COVID-Tracking e.g. tested population, negative tests, used before in [39]. **Mobility:** track people movement to several point of interests (POIs), from Google [28] and Apple [23], which can serve as a digital proxy for social distancing [3]. **Exposure:** digital signal measuring closeness between people at POIs, collected from mobile phones [10] and used before [39]. **Social Survey:** previously used [44, 39] CMU/Facebook Symptom Survey Data, which contains self-reported responses about COVID-19 symptoms of all household members.

2.2 Observations

We first study different facets of the significance of backfill in CoVDS. Using our definitions, we generate a backfill sequence for every combination of signal, observation week, and region (not all signals are available for all regions). In total, we generate *more than* 30,000 backfill sequences.

Backfill error BERR is significant. We computed BERR for the initial values, i.e., $\text{BERR}(r = 0, i, t')$, for all signals i and observation weeks t' .

Obs. 1. (BERR across signals and regions) Compute the average BERR for each signal; the median of all these averages is 32%, i.e. at least half of all signals are corrected by 32% of their initial value. Similarly in at least half of the regions the signal corrections are 280% of their initial value.

Table 1: List of features in our CoVDS

Type	Features
Patient Line-List [7, 13]	ERVisits, HospRate, +veInc, HospInc, Recovered, onVentilator, inICU
Testing [7, 13]	TestResultsInc, -veInc, Facilities
Mobility [28, 23]	RetailRec, Grocery, Parks, Transit, WorkSpace, Resident, AppleMob
Exposure [10]	DexA
Social Survey [20]	FbCLI, FbWiLi

We also found large variation of BERR. For features (Figure 1a), compare avg. BERR = 1743% of five most corrected features with 1.6% of the five least corrected features. Also, in contrast to related work that focuses on traditional surveillance data [45], perhaps unexpectedly, we found that digital indicators also have a significant BERR (average of 108%). For regions (see Figure 1b), compare 1594% of the five most corrected regions with 38% of the five least corrected regions.

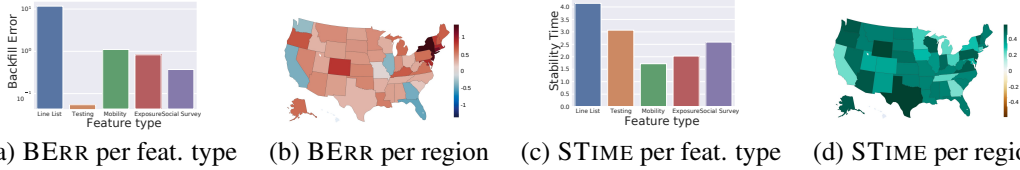


Figure 1: BERR and STIME across feature type and regions, heat maps are log scaled.

Stability time STIME is significant. A similar analysis for STIME found significant variation across signals (from 1 weeks for to 21 weeks for COVID-19, see Figure 1c) and regions (from 1.55 weeks for GA to 3.83 weeks for TX, see Figure 1d). This also impacts our target, thus, actual accuracy is not readily available which undermines real-time evaluation and decision making.

Obs. 2. (STIME of features and target) Compute the average BERR for each signal; the average of all these averages for features is around 4 weeks and for our target Deaths is around 3 weeks, i.e. on average, it takes over 3 weeks to reach the stable values of features.

Backfill sequence BSEQ patterns. There is significant similarity among BSEQs. We cluster BSEQs via K-means using Dynamic Time Warping (DTW) as pair-wise distance (as DTW can handle sequences of varying magnitude and length). We found five canonical categories of behaviors (see Figure 2), each of size roughly 11.58% of all BSEQs. Also each cluster is not defined only by signal

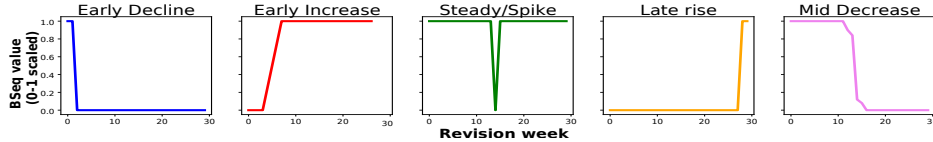


Figure 2: Five canonical backfill behaviours. Centroid BSEQ of each cluster, scaled between 0 and 1.

nor region. Hence there is a non-trivial similarity across both signals and regions.

Obs. 3. (BSEQ similarity and variety) Five canonical behaviors were observed in our backfill sequences (Figure 2). No cluster has over 21% of BSEQs from the same region, and no cluster has over 14% of BSEQs from the same signal.

Model performance vs BERR. To study the relationship between model performance (via Mean Absolute Error MAE of a prediction) and BERR, we use REVDIFFMAE: it is the difference between MAE computed against real-time target value and one against the stable target value. We analyze the top performing real-time forecasting models as per the comprehensive evaluation of all models in COVID-19 Forecast Hub [14]. YYG and UMASS-MB are mechanistic while CMU-TS and GT-DC are statistical models. The top performing ENSEMBLE is composed of all contributing models to the hub. We expect a well-trained real-time model will have higher REVDIFFMAE with larger BERR in its target.

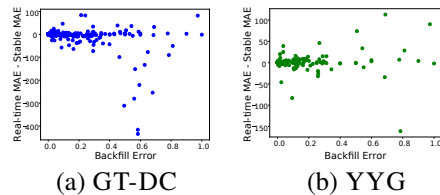


Figure 3: BERR vs model REVDIFFMAE.

However, in contrast to flu [37], here we found that more target backfill error does not necessarily mean worse performance. See Figure 3—YYG has even better performance with more revisions. This may be due to the more complex backfill activity/dependencies in COVID in comparison to the more regular seasonal flu.

Obs. 4. (Model performance and backfill) Relation between BERR and REVDIFFMAE can be non-monotonous and positively or negatively correlated depending on model and signal.

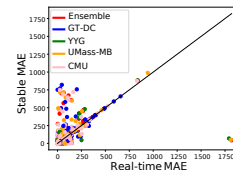


Figure 4: Real-time vs stable MAE.

Real-time target values to measure model performance: Since targets undergo revisions (5% BERR on average), we study how this BERR affects real-time evaluation of models. From Figure 4, we see that the scores are not similar with real-time scores over-estimating model accuracy. The average difference in scores is positive which implies that evaluators would overestimate models’ forecasting ability.

Obs. 5. MAE evaluated at real-time overestimates model performance by mean 9.6, with maximum for TX at 22.63.

3 Refining the future via B2F

Our observations naturally motivate improving training and evaluation aspects of *real-time* COVID-19 forecasting by leveraging revision information. Thus, we propose the following two problems. Let predictions of model M for week $t + k$ be $y(M, k)_t$. Since models are trained on *real-time* targets, $y(M, k)_t$ is the model’s estimate of target $y_{t+k}^{(t+k)}$.

k -week ahead Backfill Refinement Problem, BFRP $_k(M)$: At prediction week t , we are given a *revision dataset* $\{\mathcal{D}_{1:t'}^{(t')}\}_{t' \leq t}$, which includes our target $\mathcal{Y}_{1:t}^{(t)}$. For a model M trained on *real-time* targets, we are also given history of model’s predictions till last week $\langle y(M, k)_1, \dots, y(M, k)_{t-1} \rangle$ and prediction for current week $y(M, k)_t$. Our goal is to refine $y(M, k)_t$ to better estimate the *stable* target $y_{t+k}^{(t_f)}$, i.e. the ‘future’ of our target value at $t + k$.

Leaderboard Refinement problem, LBRP: At each week t , evaluators are given a current estimate of our target $y_t^{(t)}$ and forecasts of models submitted on week $t - k$. Our goal is to refine $y_t^{(t)}$ to \hat{y}_t , a better estimate of $y_t^{(t_f)}$, so that using \hat{y}_t as a surrogate for $y_t^{(t_f)}$ to evaluate predictions of models provides a better indicator of their actual performance (i.e., we obtain a refined leaderboard of models). Relating it to BFRP, assume a hypothetical model M_{eval} whose predictions are real-time ground truth, i.e. $y(M_{eval}, 0)_t = y_t^{(t)}, \forall t$. Then, refining M_{eval} is equivalent to refining $y_t^{(t)}$ to better estimate $y_t^{(t_f)}$ which leads to solving LBRP. Thus, LBRP is a *special case* of BFRP $_0(M_{eval})$.

Overview: We leverage observations from Section 2 to derive Back2Future (B2F), a deep-learning model that uses revision information from BSEQ to refine predictions. Obs. 1 and 2 show that real-time values of signals are poor estimates of their stable versions. Therefore, we have to leverage patterns in BSEQ of past signals and exploit cross-signal similarities (Obs. 3) to extract information from BSEQs. We also consider that the relation of models’ forecasts vs BERR of targets is complex (Obs. 4 and 5) to refine their predictions. B2F combines these ideas through its four modules:

- GRAPHGEN: Generates a signal graph (where each node corresponds to a signal in Reg \times Feat) whose edges are based on BSEQ curve similarities.
- BSEQENC: Leverages the signal graph as well as temporal dynamics of BSEQs to learn a latent representation of BSEQs using a Recurrent Graph Neural Network.
- MODELPREDEC: Encodes the history of model’s predictions, real-time value of target, and past revisions of target through a recurrent neural network.
- REFINER: Combines encodings from BSEQENC and MODELPREDEC to predict the correction to model’s real-time prediction.

In contrast to previous works that bring to attention only target BERR [37, 9], we aim to simultaneously model all BSEQ available till current week t using spatial and signal similarities in the temporal dynamics of BSEQ. Recent works that attempt to model spatial relations for COVID19 forecasting need explicitly structural data (like cross-region mobility) [32] to generate graph or use attention over temporal patterns of all region’s death trends. B2F, in contrast, directly models the structural information of signal graph (containing feature nodes from each region) using BSEQ similarities.

Thus, our goal is to first generate useful latent representations for each signal based on BSEQ revision information of that feature as well as features that have shown similar revision patterns in the past. Due to large number of signals that covers all regions, we cannot model relation between every pair using fully connected modules or attention similar to [24]. Therefore, we first construct a sparse graph between signals based on past BSEQ similarities. Then we inject this similarity information using Graph Convolutional Networks (GCNs) and combine it with deep sequential models to model temporal dynamics of BSEQ of each signal while combining information from BSEQ s of signals in the neighborhood of the graph. Further, we use these latent representations and leverage the past

history of a model M 's predictions to refine its prediction. Thus, B2F solves $\text{BFRP}_k(M)$ assuming M is a black box, accessing only its past forecasts. Our training process, that involves pre-training on model-agnostic auxiliary task, greatly improves training time for refining any given model M .

Next we describe each of the components of B2F in detail. For the rest of this section, we will assume that we are forecasting k weeks ahead given data till current week t .

GRAPHGEN. It generates an undirected signal graph $G_t = (V, E_t)$ whose edges represent similarity in BSEQs between signals, where vertices $V = \mathcal{F} = \text{Reg} \times \text{Feat}$. We measure similarity using DTW distance due to reasons described in Section 2. We compute the sum of DTW distances of BSEQs for each pair of nodes summed over $t' \in \{1, 2, \dots, t-5\}$. We threshold t' till $t-5$ to make the BSEQs to be of reasonable length (at least 5) to capture temporal similarity without discounting too many BSEQs. The top τ node pairs with lowest total DTW distance are assigned an edge.

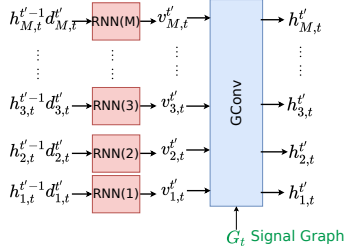


Figure 5: BSEQENC Recurrent Module

While we can model backfill sequences for each signal independently using a recurrent neural network, this doesn't capture the behavioral similarity of BSEQ across signals. Using a fully-connected recurrent neural network which considers all possible interactions between signals also may not learn from the similarity information due to the sheer number of signals ($50 \times 21 = 1050$) while greatly increasing the parameters of the model. Thus, we utilize the structural prior of graph G_t generated by GRAPHGEN and train an autoregressive model BSEQENC which consists of graph recurrent neural network to encode a latent representation for each of back-

fill sequence in $B_t = \{\text{BSEQ}(i, t) : i \in \mathcal{F}\}$. At week t , BSEQENC is first pre-trained and then it is fine-tuned for a specific model M (more details later in this section). Our encoding process is in Figure 5. Let $\text{BSEQ}_{t'+r}(i, t')$ be first $r+1$ values of $\text{BSEQ}(i, t')$ (till week $t'+r$). For a past week t' and revision week r , we denote $h_{i,t'}^{(t')}$ $\in \mathbb{R}^m$ to be the latent encoding of $\text{BSEQ}_{t'}(i, t')$ where $t'_r = t' + r$ and $t' \leq t'_r \leq t$. We initialize $h_{i,t'}^{(0)}$ for any observation week t' to be a learnable parameter $h_i^{(0)} \in \mathbb{R}^m$ specific to signal i . For each week t'_r we combine latent encoding $h_{i,t'}^{(t'_r-1)}$ and signal value $d_{i,t'}^{(t'_r)}$ using a GRU (Gated Recurrent Unit) [11] cell to get the intermediate embedding $v_{i,t'}^{(t'_r)}$. Then, we leverage the signal graph G_t and pass the embeddings $\{v_{i,t'}^{(t'_r)} : i \in \mathcal{F}\}$ through a Graph Convolutional layer [25] to get $h_{i,t'}^{(t'_r)}$:

$$v_{i,t'}^{(t'_r)} = \text{GRU}_{\text{BE}}(d_{i,t'}^{(t'_r)}, h_{i,t'}^{(t'_r-1)}), \quad \{h_{i,t'}^{(t'_r)}\}_{i \in \mathcal{F}} = \text{GConv}(G_t, \{v_{i,t'}^{(t'_r)}\}_{i \in \mathcal{F}}). \quad (1)$$

Thus, $h_{i,t'}^{(t'_r)}$ contains information from $\text{BSEQ}_{t'_r}(i, t')$ and structural priors from G_t . Using $h_{i,t'}^{(t'_r)}$, BSEQENC predicts the value $d_{i,t'}^{(t'_r+1)}$ by passing through a 2-layer feed-forward network FFN_i : $\hat{d}_{i,t'}^{(t'_r+1)} = \text{FFN}_i(h_{i,t'}^{(t'_r)})$. During inference, we only have access to real-time values of signals for the current week. We autoregressively predict $h_{i,t}^{(t+l)}$ for each signal by initially passing $\{d_{i,t}^{(t)}\}_{i \in \mathcal{F}}$ through BSEQENC and using the output $\{\hat{d}_{i,t}^{(t+1)}\}_{i \in \mathcal{F}}$ as input for BSEQENC. Iterating this l times we get $\{h_{i,t}^{(t+l)}\}_{i \in \mathcal{F}}$ along with $\{\hat{d}_{i,t}^{(t+l)}\}_{i \in \mathcal{F}}$ where l is a hyperparameter.

MODELPREDENC. To learn from history of a model's predictions and its relation to target revisions, MODELPREDENC encodes the history of model's predictions, previous real-time targets, and revised (up to current week) targets using a Recurrent Neural Network. Given a model M , for each observation week $t' \in \{1, 2, \dots, t-1-k\}$, we concatenate the model's predictions $y(M, k)_{t'}$, real-time target $y_{t'+k}^{(t'+k)}$ as seen on observation week t' and revised target $y_{t'+k}^{(t)}$ as $C_{t'}^t = y(M, k)_{t'} \oplus y_{t'+k}^{(t'+k)} \oplus y_{t'+k}^{(t)}$, where \oplus is the concatenation operator. A GRU is used to encode the sequence $\{C_1^{(t)}, \dots, C_{t-1-k}^{(t)}\}$:

$$\{z_1^{(t)}, \dots, z_{t-1-k}^{(t)}\} = \text{GRU}_{\text{ME}}(\{C_1^{(t)}, \dots, C_{t-1-k}^{(t)}\}) \quad (2)$$

REFINER. It leverages the information from above three modules of B2F to refine model M 's prediction for current week $y(M, k)_t$. Specifically, it receives the latent encodings of signals $\{h_{i,t}^{(t+l)}\}_{i \in \mathcal{F}}$ from BSEQENC, $z_{t-k-1}^{(t)}$ from MODELPREDENC, and the model's prediction $y(M, k)_t$ for week t .

BSEQ encoding from different signals may have variable impact on refining the signal since a few signals may not very useful for current week's forecast (e.g., small revisions in mobility signals may not be important in some weeks). Moreover, because different models use signals from CoVDS differently, we may need to focus on some signals over others to refine its prediction. Therefore, we first take attention over BSEQ encodings from all signals $\{h_{i,t}^{(t+l)}\}_{i \in \mathcal{F}}$ w.r.t $y(M, k)_t$. We use multiplicative attention mechanism with parameter $w \in \mathbb{R}^m$ based on [43]:

$$\alpha_i = \text{softmax}_i(y(M, k)_t w_{\bar{h}}^T h_{i,t}^{t+l}), \quad \bar{h}^{(t)} = \sum_{i \in \mathcal{F}} (\alpha_i h_{i,t}^{t+l}). \quad (3)$$

Finally we combine $\bar{h}^{(t)}$ and $z_{t-k-1}^{(t)}$ through a two layer feed-forward layer FNN_{RF} which outputs a 1-dim value followed by tanh activation to get the correction $\gamma_t \in [-1, 1]$ i.e., $\gamma_t = \tanh(\text{FNN}_{\text{RF}}(\bar{h}^{(t)} \oplus z_{t-k-1}^{(t)}))$. Finally, the refined prediction is $y^*(M, K)_t = (\gamma + 1)y(M, K)_t$. Note that we limit the correction by B2F by at-most the magnitude of model's prediction because the average BERR of targets is 4.9% and less than 0.6% of them have BERR over 1. Therefore, we limit the refinement of prediction to this range.

Training: There are two steps of training involved for B2F: 1) model agnostic autoregressive BSEQ prediction task to pre-train BSEQENC; 2) model specific training for BFRP.

Autoregressive BSEQ prediction: Pre-training on auxillary tasks to improve the quality of latent embedding is a well-known technique for deep learning methods [18, 35]. We pre-train BSEQENC to predict the next values of backfill sequences $\{x_{t',i}^{(t'+1)}\}_{i \in \mathcal{F}}$. Note that we only use BSEQ sequences $\{\text{BSEQ}_t(t', i)\}_{i \in \mathcal{F}, t' < t}$ available till current week t for training BSEQENC. The training procedure in itself is similar to Seq2Seq prediction problems [42] where for initial epochs we use the ground truth inputs at each step (teacher forcing) and then transition to using output predictions of previous time step by recurrent module as input to next time step. Once we pre-train BSEQENC, we can use it for BFRP as well as LBRP for current week t for any model M . Fine-tuning usually takes less than half the epochs required for pre-training enabling quick refinement of multiple models in parallel.

Model specific end-to-end training: Given the pre-trained BSEQENC, we train, end-to-end, the parameters of all modules of B2F. The training set consists of past model predictions $\langle y(M, k)_1, y(M, k)_2, \dots, y(M, k)_{t-1} \rangle$ and backfill sequences $\{\text{BSEQ}_t(t', i)\}_{i \in \mathcal{F}, t' \leq t}$. For datapoint $y(M, k)_{t'}$ of week $t' < t - k$, we input backfill sequences of signals whose observation week is t' into BSEQENC to get latent encodings $\{h_{i,t'}^{(t)}\}_{i \in \mathcal{F}}$. We also derive $z_{t'}^{(t)}$ from MODELPREDENC and finally REFINER ingests $z_{t'}^{(t)}$, $\{h_{i,t'}^{(t)}\}_{i \in \mathcal{F}}$ and $y(M, k)_{t'}$ to get $\gamma_{t'}$. Overall, we optimize the loss function: $\mathcal{L}^{(t)} = \sum_{i=1}^{t-k-1} (\gamma_{t'} y(M, k)_{t'} - y_{t'+k}^{(t)})^2$. Following real-time forecasting, we train B2F each week from scratch (including pre-training). Throughout training and forecasting for week t , we use G_t as input to BSEQENC since it capture average similarities in BSEQs till current week t .

4 Back2Future Experimental Results

In this section, we describe a detailed empirical study to evaluate the effectiveness of our framework B2F. All experiments were run in an Intel i7 4.8 GHz CPU with Nvidia Tesla A4 GPU. The model typically takes around 1 hour to train for all regions. Supplementary contains additional details and results (code, CoVDS dataset, all hyperparameters and results for $k = 1$).

Setup: We perform real-time forecasting of COVID-19 related mortality (Deaths) for 50 US states from beginning of June 2020 (referred as week 1) to end of December 2020 (referred as week T'). For each week t , we only use the CoVDS dataset available till current week t (including BSEQs for all signals revised till t) for training. As described in Section 3, for each week, we first pre-train BSEQENC on BSEQ data and then train all components of B2F for each model we aim to refine. Then, we predict the forecasts $y^*(M, k)_t$ for each model M . We observed that setting hyperparameter $\tau = c|\mathcal{F}|$ where $c \in \{2, 3, 4, 5\}$ provided best results. Note that τ influences the

sparsity of the graph as well as efficiency of model since sparser graphs lead to fast inference across GConv layers. We also found setting $l = 5$ provided best performance.

Evaluation: We evaluate the refined prediction $y^*(M, K)_t$ against the most revised version of the target, i.e. $y_{t+k}^{(t_f)}$. In our case, t_f is second week of Feb 2021. For evaluation, we use standard metrics in this domain [37, 1]. Let absolute error of prediction $e(M, k)_t = |y_{t+k}^{(t_f)} - y^*(M, K)_t|$ for a week t and model M . We use (a) Mean Absolute Error $MAE(M) = \frac{1}{T'} \sum_{i=1}^{T'} |e(M, k)_t|$ and (b) Mean Absolute Percentage Error $MAPE = \frac{1}{T'} \sum_{i=1}^{T'} e(M, k)_t / |y_{t+k}^{(t_f)}|$.

Candidate models: We focus on refining/rectifying the top models from the COVID-19 Forecast Hub described in Section 2; these represent different variety of statistical and mechanistic models.

Table 2: B2F consistently refines all models. % improvements in MAE and MAPE scores averaged over all regions from May 2020 to Dec 2020

Cand. Model	Refining Model	k=2		k=3		k=4	
		MAE	MAPE	MAE	MAPE	MAE	MAPE
ENSEMBLE	FFNREG	-0.35	-0.12	0.48	-0.29	0.81	0.36
	PREDRNN	-2.23	-1.57	-1.51	-3.78	-1.13	-2.36
	BSEQREG2	-1.45	-2.73	-1.74	-3.21	-5.2	-4.78
	BSEQREG	1.42	0.37	0.37	0.22	0.72	0.28
GT-DC	B2F	5.18	5.47	3.64	3.9	3.61	6.3
	FFNREG	-2.42	-1.51	-2.04	-6.07	-1.86	-0.49
	PREDRNN	-3.02	-3.41	-2.62	-3.95	-2.81	-3.26
	BSEQREG2	2.24	3.51	2.31	2.42	1.6	0.57
YYG	BSEQREG	2.13	3.84	3.6	3.55	1.42	2.27
	B2F	12.68	12.59	11.42	10.67	9.64	8.97
	FFNREG	-2.08	-1.34	-4.62	-3.89	-1.37	-3.06
	PREDRNN	-3.84	-6.99	-5.57	-4.16	-9.29	-5.81
UMASS-MB	BSEQREG2	-1.25	-0.7	-2.57	-3.72	-6.65	-5.45
	BSEQREG	-1.78	-2.26	-1.99	-1.53	-0.61	-0.43
	B2F	8.84	5.98	7.04	7.64	6.8	5.27
	FFNREG	-3.25	-5.74	-2.16	-3.17	-1.44	-4.84
CMU-TS	PREDRNN	-8.2	-7.54	-5.19	-7.82	-5.99	-7.43
	BSEQREG2	-2.16	-1.88	-2.13	-0.67	-2.29	-2.31
	BSEQREG	1.58	0.86	-1.26	0.45	0.06	0.03
	B2F	5.21	4.92	3.25	4.74	3.94	3.49
CMU-TS	FFNREG	-5.24	-4.93	-2.87	-1.95	-3.19	-6.7
	PREDRNN	-8.17	-8.21	-3.32	-6.3	-3.75	-9.1
	BSEQREG2	-0.67	-0.57	-0.73	-0.19	-0.38	-0.12
	BSEQREG	1.46	1.05	2.74	2.47	2.11	2.84
	B2F	8.75	10.48	5.84	7.62	6.93	6.28

Baselines: Due to the novel problem, there are no standard baselines. (a) FFNREG: train a FFN for regression task that takes as inputs model’s prediction and real-time target to predict stable target. (b) PREDRNN: use the MODELPREDEC architecture and append a linear layer that takes encodings from MODELPREDEC and model’s prediction and train it to refine the prediction. (c) BSEQREG: similarly, only use BSEQENC architecture and append a linear layer that takes encodings from BSEQENC and model’s prediction to predict stable target.

(d) BSEQREG2: similar to BSEQREG but remove the graph convolutional layers and retain only RNNs. Note that FFNREG and PREDRNN do not use revision data. BSEQREG and BSEQREG2 don’t use past predictions of the model.

Refining real-time model-predictions: See Table 2. We compare the mean percentage improvement (i.e., decrease) in MAE and MAPE scores of refined predictions over model’s predictions on stable targets over 50 US states².

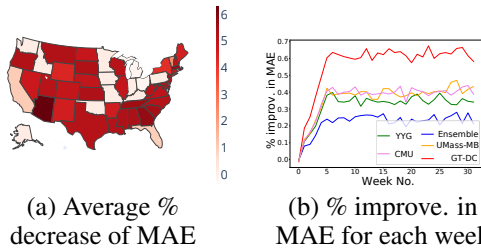


Figure 6: (a) B2F refines ENSEMBLE predictions significantly for most states. (b) efficacy of B2F ramps up within 6 weeks of revision data.

First, we observe that B2F is the only method, compared to baselines, that improves scores for *all* candidate models showcasing the necessity of incorporating backfill information (unlike FFNREG and PREDRNN) and model prediction history (unlike BSEQREG and BSEQREG2).

We achieve impressive avg. improvements of 6.65% and 6.95% in MAE and MAPE respectively with improvements decreasing with increasing k . For all candidate models, B2F shows improvement over 10% in over 25 states

²Results described are statistically significance due to Wilcox signed rank test ($\alpha = 0.05$) over 5 runs

and over 15% in 5 states (NJ, LA, GA, CT, MD). Thanks to B2F refinement, CMU-TS and GT-DC which are ranked 3th and 4th in COVID-19 Forecast Hub, now are able to outperform all the models in the hub (except for ENSEMBLE) with impressive 7.17% and 4.13% improvements in MAE respectively. UMASS-MB, ranked 2nd, is improved by 11.24%. B2F also improves ENSEMBLE, which is the current best performing model of the hub, by 3.6% - 5.18% making B2F refined ENSEMBLE *the best COVID-19 forecasting model*. Notably, B2F improves ENSEMBLE by over 5% in 38 states, with IL and TX experiencing over 15% improvement.

Rectifying real-time model-evaluation: We evaluate the efficacy of B2F in rectifying the real-time evaluation scores for LBRP problem. We noted in Obs 5 that real-time MAE was lower than stable MAE by 9.6 on average. The difference between B2F rectified estimates MAE stable MAE was reduced to 4.4, a 51.7% decrease (Figure 7). This results in increased MAE scores across most regions towards stable estimates. Eg: We reduce the MAE difference in large highly populated states such as GA by 26.1% (from 22.52 to 16.64) and TX by 90% (from 10.8 to 1.04) causing increase in MAE scores from real-time estimates by 5.88 and 9.4 respectively.

Refinement as function of data availability: Note that during the initial weeks of the pandemic, we have access to very little revision data both in terms of length and number of BSEQ. So we evaluate the mean performance improvement for each week across all regions (Figure 6b). B2F’s performance ramps up and quickly stabilizes in just 6 weeks. Since signals need around 4 weeks (Obs 2) to stabilize, this ramp up time is impressive. Thus, B2F *needs small amount of revision data from to improve model performance*.

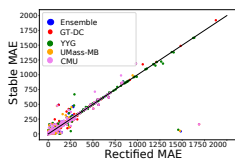


Figure 7: B2F *rectified MAE are closer to stable MAE*

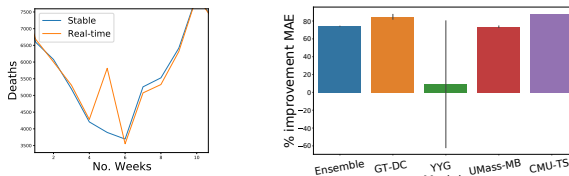
B2F adapts to anomalies During real-time forecasting it is important for models to be robust to anomalous data revisions. This is especially true during initial stages of epidemic when data collection is not full streamlined and may experience large revisions. Consider observation week 5 (first week of June) where there was an abnormally large revision to deaths nationwide (Figure 8a) when the BERR was 48%. B2F still provided significant improvements for most model predictions (Figure 8b). Specifically ENSEMBLE’s predictions are refined to be up to 74.2% closer to stable target.

5 Conclusion

We introduced and studied the challenging multi-variate backfill problem using COVID-19 as an example, introducing new problems to this space. We presented Back2Future (B2F), the novel deep-learning method to model this phenomena, which exploits our observations of cross-signal similarities using Graph Recurrent Neural Networks to refine predictions and rectify evaluations for a wide range of models.

Our extensive experiments showed that leveraging similarity among backfill patterns via our proposed method leads to impressive improvements in all the top models at the CDC COVID-19 Forecast Hub. In fact, we improved even the best performing model up to 15%.

As future work, our work can potentially help improve data collection, e.g. we pointed systematic differences between regions, which can also have implications for equity due to uneven reporting capabilities. We emphasize that we used the CoVDS dataset as is, but our characterization can be helpful for anomaly detection [14, 22]. We can also study how backfill can effect uncertainty calibration and quantification in time-series analysis [41, 47]. Another direction can be to explore situations where revision history is not temporally uniform across all features due revisions of different frequency or aperiodic revisions which B2F currently can not ingest without pre-processing. Although our dataset is public/anonymized without any sensitive patient information, there might be limited potential for misuse of our algorithms and/or data sources.



(a) Revision of US deaths on week 5 (b) % decrease in MAE due to B2F refinement on week 5 targets

Figure 8: B2F *adapts to abnormally high revisions*

6 Acknowledgements

This paper is based on work partially supported by the NSF (Expeditions CCF-1918770, CAREER IIS-2028586, RAPID IIS-2027862, Medium IIS-1955883, CCF-2115126), CDC MInD program, ORNL, and funds/computing resources from Georgia Tech.

References

- [1] Bijaya Adhikari, Xinfeng Xu, Naren Ramakrishnan, and B Aditya Prakash. “Epideep: Exploiting embeddings for epidemic forecasting”. In: *Proceedings of the 25th ACM SIGKDD International Conference on Knowledge Discovery & Data Mining*. 2019, pp. 577–586.
- [2] Nick Altieri, Rebecca L Barter, James Duncan, Raaz Dwivedi, Karl Kumbier, Xiao Li, Robert Netzorg, Briton Park, Chandan Singh, Yan Shuo Tan, Tiffany Tang, Yu Wang, Chao Zhang, and Bin Yu. “Curating a COVID-19 Data Repository and Forecasting County-Level Death Counts in the United States”. In: *Harvard Data Science Review* (Feb. 8, 2021). <https://hdsr.mitpress.mit.edu/pub/p6isyf0g>. DOI: 10.1162/99608f92.1d4e0dae. URL: <https://hdsr.mitpress.mit.edu/pub/p6isyf0g>.
- [3] Sercan Arik, Chun-Liang Li, Jinsung Yoon, Rajarishi Sinha, Arkady Epshteyn, Long Le, Vikas Menon, Shashank Singh, Leyou Zhang, Martin Nikoltshev, et al. “Interpretable Sequence Learning for Covid-19 Forecasting”. In: *Advances in Neural Information Processing Systems* 33 (2020).
- [4] Matthew Biggerstaff, Michael Johansson, David Alper, Logan C Brooks, Prithwish Chakraborty, David C Farrow, Sangwon Hyun, Sasikiran Kandula, Craig McGowan, Naren Ramakrishnan, et al. “Results from the second year of a collaborative effort to forecast influenza seasons in the United States”. In: *Epidemics* 24 (2018), pp. 26–33.
- [5] Logan C. Brooks, David C. Farrow, Sangwon Hyun, Ryan J. Tibshirani, and Roni Rosenfeld. “Nonmechanistic forecasts of seasonal influenza with iterative one-week-ahead distributions”. In: *PLOS Computational Biology* 14.6 (June 2018). Ed. by Cecile Viboud, e1006134. ISSN: 1553-7358. DOI: 10.1371/journal.pcbi.1006134. URL: <https://dx.plos.org/10.1371/journal.pcbi.1006134> (visited on 05/02/2019).
- [6] Andrea Carriero, Michael P Clements, and Ana Beatriz Galvão. “Forecasting with Bayesian multivariate vintage-based VARs”. In: *International Journal of Forecasting* 31.3 (2015), pp. 757–768.
- [7] CDC. *Coronavirus Disease 2019 (COVID-19)*. 2020. URL: <https://www.cdc.gov/coronavirus/2019-ncov/cases-updates/>.
- [8] Prithwish Chakraborty, Pejman Khadivi, Bryan Lewis, Aravindan Mahendiran, Jiangzhuo Chen, Patrick Butler, Elaine O Nsoesie, Sumiko R Mekaru, John S Brownstein, Madhav V Marathe, et al. “Forecasting a moving target: Ensemble models for ILI case count predictions”. In: *Proceedings of the 2014 SIAM international conference on data mining*. SIAM. 2014, pp. 262–270.
- [9] Prithwish Chakraborty, Bryan Lewis, Stephen Eubank, John S. Brownstein, Madhav Marathe, and Naren Ramakrishnan. “What to know before forecasting the flu”. In: *PLoS Computational Biology* 14.10 (Oct. 2018). ISSN: 1553-734X. DOI: 10.1371/journal.pcbi.1005964. URL: <https://www.ncbi.nlm.nih.gov/pmc/articles/PMC6193572/> (visited on 08/16/2020).
- [10] Judith A Chevalier, Jason L Schwartz, Yihua Su, Kevin R Williams, et al. *Measuring Movement and Social Contact with Smartphone Data: A Real-time Application to COVID-19*. Tech. rep. Cowles Foundation for Research in Economics, Yale University, 2021.
- [11] Kyunghyun Cho, B. V. Merriënboer, Dzmitry Bahdanau, and Yoshua Bengio. “On the Properties of Neural Machine Translation: Encoder-Decoder Approaches”. In: *ArXiv abs/1409.1259* (2014).
- [12] Michael P Clements and Ana Beatriz Galvão. “Data revisions and real-time forecasting”. In: *Oxford Research Encyclopedia of Economics and Finance*. 2019.
- [13] COVID-Tracking. *The COVID Tracking Project*. 2020. URL: <https://covidtracking.com>.

- [14] Estee Y Cramer, Velma K Lopez, Jarad Niemi, Glover E George, Jeffrey C Cegan, Ian D Dettwiller, William P England, Matthew W Farthing, Robert H Hunter, Brandon Lafferty, et al. “Evaluation of individual and ensemble probabilistic forecasts of COVID-19 mortality in the US”. In: *medRxiv* (2021).
- [15] Dean Croushore. “Forecasting with real-time data vintages”. In: *The Oxford handbook of economic forecasting* (2011), pp. 247–267.
- [16] Aron Culotta. “Towards detecting influenza epidemics by analyzing Twitter messages”. In: *Proceedings of the first workshop on social media analytics*. 2010, pp. 115–122.
- [17] Songgaojun Deng, Shusen Wang, Huzefa Rangwala, Lijing Wang, and Yue Ning. “Cola-GNN: Cross-location Attention based Graph Neural Networks for Long-term ILI Prediction”. In: *Proceedings of the 29th ACM International Conference on Information & Knowledge Management*. 2020, pp. 245–254.
- [18] J. Devlin, Ming-Wei Chang, Kenton Lee, and Kristina Toutanova. “BERT: Pre-training of Deep Bidirectional Transformers for Language Understanding”. In: *NAACL-HLT*. 2019.
- [19] Jeremy Ginsberg, Matthew H Mohebbi, Rajan S Patel, Lynnette Brammer, Mark S Smolinski, and Larry Brilliant. “Detecting influenza epidemics using search engine query data”. In: *Nature* 457.7232 (2009), pp. 1012–1014.
- [20] Delphi Group. *COVID Symptom Survey*. <https://cmu-delphi.github.io/delphi-epidata/symptom-survey/>. 2021.
- [21] Inga Holmdahl and Caroline Buckee. “Wrong but Useful — What Covid-19 Epidemiologic Models Can and Cannot Tell Us”. In: *NEJM* 383.4 (2020), pp. 303–305.
- [22] Hajar Homayouni, Indrakshi Ray, Sudipto Ghosh, Shlok Gondalia, and Michael G Kahn. “Anomaly Detection in COVID-19 Time-Series Data”. In: *SN Computer Science* 2.4 (2021), pp. 1–17.
- [23] Apple Inc. *Apple Mobility Trends Reports*. 2020. URL: www.apple.com/covid19/mobility.
- [24] Xiaoyong Jin, Yu-Xiang Wang, and Xifeng Yan. “Inter-Series Attention Model for COVID-19 Forecasting”. In: *ArXiv abs/2010.13006* (2020).
- [25] Thomas N Kipf and Max Welling. “Semi-supervised classification with graph convolutional networks”. In: *arXiv preprint arXiv:1609.02907* (2016).
- [26] Vasileios Lampos, Tijn De Bie, and Nello Cristianini. “Flu detector-tracking epidemics on Twitter”. In: *Joint European conference on machine learning and knowledge discovery in databases*. Springer. 2010, pp. 599–602.
- [27] Shenghua Liu, Bryan Hooi, and Christos Faloutsos. “Holoscope: Topology-and-spike aware fraud detection”. In: *Proceedings of the 2017 ACM on Conference on Information and Knowledge Management*. 2017, pp. 1539–1548.
- [28] Google LLC. *Google COVID-19 Community Mobility Reports*. 2020. URL: <https://www.google.com/covid19/mobility/>.
- [29] C Jessica E Metcalf and Justin Lessler. “Opportunities and challenges in modeling emerging infectious diseases”. In: *Science* 357.6347 (2017), pp. 149–152.
- [30] Dave Osthus, Ashlynn R Daughton, and Reid Priedhorsky. “Even a good influenza forecasting model can benefit from internet-based nowcasts, but those benefits are limited”. In: *PLoS computational biology* 15.2 (2019), e1006599.
- [31] Dave Osthus, James Gattiker, Reid Priedhorsky, Sara Y Del Valle, et al. “Dynamic Bayesian influenza forecasting in the United States with hierarchical discrepancy (with discussion)”. In: *Bayesian Analysis* 14.1 (2019), pp. 261–312.
- [32] G. Panagopoulos, Giannis Nikolentzos, and M. Vazirgiannis. “United We Stand: Transfer Graph Neural Networks for Pandemic Forecasting”. In: *ArXiv abs/2009.08388* (2020).
- [33] George Panagopoulos, Giannis Nikolentzos, and Michalis Vazirgiannis. “Transfer Graph Neural Networks for Pandemic Forecasting”. In: *Proceedings of the AAAI Conference on Artificial Intelligence*. 2021.
- [34] Sen Pei, Sasikiran Kandula, Wan Yang, and Jeffrey Shaman. “Forecasting the spatial transmission of influenza in the United States”. In: *Proceedings of the National Academy of Sciences* 115.11 (2018), pp. 2752–2757.
- [35] Alec Radford, Karthik Narasimhan, Tim Salimans, and Ilya Sutskever. “Improving language understanding with unsupervised learning”. In: (2018).

- [36] Prashant Rangarajan, Sandeep K Mody, and Madhav Marathe. “Forecasting dengue and influenza incidences using a sparse representation of Google trends, electronic health records, and time series data”. In: *PLoS computational biology* 15.11 (2019), e1007518.
- [37] Nicholas G. Reich, Logan C. Brooks, Spencer J. Fox, Sasikiran Kandula, Craig J. McGowan, Evan Moore, Dave Osthus, Evan L. Ray, Abhinav Tushar, Teresa K. Yamana, Matthew Biggerstaff, Michael A. Johansson, Roni Rosenfeld, and Jeffrey Shaman. “A collaborative multiyear, multimodel assessment of seasonal influenza forecasting in the United States”. eng. In: *Proceedings of the National Academy of Sciences of the United States of America* 116.8 (2019), pp. 3146–3154. ISSN: 1091-6490. DOI: 10.1073/pnas.1812594116.
- [38] Alexander Rodríguez, Nikhil Muralidhar, Bijaya Adhikari, Anika Tabassum, Naren Ramakrishnan, and B Aditya Prakash. “Steering a Historical Disease Forecasting Model Under a Pandemic: Case of Flu and COVID-19”. In: *Proceedings of the AAAI Conference on Artificial Intelligence*. 2021.
- [39] Alexander Rodríguez, Anika Tabassum, Jiaming Cui, Jiajia Xie, Javen Ho, Pulak Agarwal, Bijaya Adhikari, and B. Aditya Prakash. “DeepCOVID: An Operational Deep Learning-Driven Framework for Explainable Real-Time COVID-19 Forecasting”. In: *Proceedings of the AAAI Conference on Artificial Intelligence*. 2021.
- [40] Jeffrey Shaman and Alicia Karspeck. “Forecasting seasonal outbreaks of influenza”. In: *Proceedings of the National Academy of Sciences* 109.50 (2012), pp. 20425–20430.
- [41] Gautam Singh, Jaesik Yoon, Youngsung Son, and Sungjin Ahn. “Sequential neural processes”. In: *Advances in Neural Information Processing Systems* 32 (2019).
- [42] Ilya Sutskever, Oriol Vinyals, and Quoc V. Le. “Sequence to Sequence Learning with Neural Networks”. In: *NIPS*. 2014.
- [43] Ashish Vaswani, Noam M. Shazeer, Niki Parmar, Jakob Uszkoreit, Llion Jones, Aidan N. Gomez, Lukasz Kaiser, and Illia Polosukhin. “Attention is All you Need”. In: *ArXiv abs/1706.03762* (2017).
- [44] Peng-Wei Wang, Wei-Hsin Lu, Nai-Ying Ko, Yi-Lung Chen, Dian-Jeng Li, Yu-Ping Chang, and Cheng-Fang Yen. “COVID-19-related information sources and the relationship with confidence in people coping with COVID-19: Facebook survey study in Taiwan”. In: *Journal of medical Internet research* 22.6 (2020), e20021.
- [45] Shihao Yang, Mauricio Santillana, and Samuel C Kou. “Accurate estimation of influenza epidemics using Google search data via ARGO”. In: *Proceedings of the National Academy of Sciences* 112.47 (2015), pp. 14473–14478.
- [46] Changchang Yin, Ruoqi Liu, Dongdong Zhang, and Ping Zhang. “Identifying sepsis subphenotypes via time-aware multi-modal auto-encoder”. In: *Proceedings of the 26th ACM SIGKDD international conference on knowledge discovery & data mining*. 2020, pp. 862–872.
- [47] Jaesik Yoon, Gautam Singh, and Sungjin Ahn. “Robustifying Sequential Neural Processes”. In: *Proceedings of the 37th International Conference on Machine Learning*. Ed. by Hal Daumé III and Aarti Singh. Vol. 119. Proceedings of Machine Learning Research. PMLR, 13–18 Jul 2020, pp. 10861–10870. URL: <http://proceedings.mlr.press/v119/yon20c.html>.
- [48] Qian Zhang, Nicola Perra, Daniela Perrotta, Michele Tizzoni, Daniela Paolotti, and Alessandro Vespignani. “Forecasting seasonal influenza fusing digital indicators and a mechanistic disease model”. In: *Proceedings of the 26th International Conference on World Wide Web*. International World Wide Web Conferences Steering Committee. 2017, pp. 311–319.
- [49] Indre Žliobaite. “Change with delayed labeling: When is it detectable?” In: *2010 IEEE International Conference on Data Mining Workshops*. IEEE. 2010, pp. 843–850.

Appendix for Back2Future: Leveraging Backfill Dynamics for Improving Real-time Predictions in Future

Code for B2F and CoVDS dataset is publicly available ³. Please refer to the README in code repository for more details.

A Additional Related work

Epidemic forecasting. Broadly two classes of approaches have been devised: traditional mechanistic epidemiological models [40, 48], and the fairly newer statistical approaches [5, 1, 31], which have become among the top performing ones for multiple forecasting tasks [37].

Statistical models have been helpful in using digital indicators such as search queries [19, 45] and social media [16, 26], that can give more lead time than traditional surveillance methods. Recently, deep learning models have seen much work. They can use heterogeneous and multimodal data and extract richer representations, including for modeling spatio-temporal dynamics [1, 17] and transfer learning [33, 38]. Our work can be thought of refining any model (mechanistic/statistical) in this space.

Revisions and backfill. The topic of revisions has not received as much attention, with few exceptions. In epidemic forecasting, a few papers have either (a) mentioned about the ‘backfill problem’ and its effects on performance [9, 39, 2, 36] and evaluation [37]; or (b) proposed to address the problem via simple models like linear regression [8] or ‘backcasting’ [5] the observed targets. However they focus only on revisions in the *target*, and study only in context of influenza forecasting, which is substantially less noisy and more regular than forecasting for the novel COVID-19 pandemic. [37] proposed a framework to study how backfill affects the evaluation of multiple models, but it is limited to label backfill and flu forecasting, which is less chaotic than the COVID scenario that we study. [12] surveys several domain-specific [6] or essentially linear techniques in economics for data revision/correction behavior of the source of several macroeconomic indicators [15]. In contrast, we study the more challenging problem of multi-variate backfill for both features and targets and show how to leverage our insights for more general neural framework to *improve* both model predictions and evaluation.

B Nature of backfill dynamics (More details)

B.1 Considering Delay in reporting

Let current week be t . Due to delay in reporting, the first observed value for some signals could be delayed by 1 to 3 weeks. For instance, BSEQ(i, t) may not have the first δ_i values due to δ_i weeks delay in reporting. In such cases, for analysis of BSEQ in Section 2, we take $d_{i,t}^{t+\delta_i}$ as the first value of BSEQ(i, t) = $\langle d_{i,t}^{t+\delta_i}, d_{i,t}^{t+\delta_i+1}, \dots, d_{i,t}^{t_f} \rangle$. Subsequently, BERR(r, i, t) is only defined for $r > \delta_i$ as $\text{BERR}(r, i, t) = \frac{|d_{i,t}^{(t+r)} - d_{i,t}^{t_f}|}{|d_{i,t}^{t_f}|}$.

Real-time forecasting As mentioned in main paper, we handle delay in reporting real time data by approximating from previous week. During real-time forecasting, we cannot wait for δ_i weeks to get the first value of a signal. Therefore, we replace $d_{i,t}^{(t)}$ with the most revised value of last week for which the signal is available. Let $t' < t$ is the last week before t for which we have $d_{i,t'}^{(t)}$. Then, we use $d_{i,t'}^{(t)}$ in place of unavailable $d_{i,t}^{(t)}$. Note that such cases of missing initial value during real-time forecasting is very uncommon.

B.2 Description of canonical backfill behaviours

We saw in Observation 3 that clustering BSEQs resulted in 5 canonical behaviours. The behaviors of these clusters as shown in Figure 2 can be described as:

³Link to code and dataset: <https://github.com/AdityaLab/Back2Future>

1. **Early Decrease:** BSEQ values stabilizes quickly (within a week) to a lower stable value.
2. **Early Increase:** BSEQ values increase in 2 to 5 weeks and stabilize.
3. **Steady/Spike:** BSEQ values either remain constant (no significant revision) or due to reporting errors there may be anomalous values in between. (E.g., for a particular week in middle of BSEQ the signals are revised to 0 due to reporting error).
4. **Late Increase:** BSEQ values increase and stabilize very late during revision.
5. **Mid Decrease:** BSEQ values change and stabilize after 8 to 10 weeks of revision.

B.3 Correlation between BERR and model performance

In Observation 4, we found that models differ in how their performance is impacted by BERR on the label and found that relationship between BERR and difference in MAE (REVDIFFMAE) was varied across models with some models (YYG) even showing positive correlation between BERR and REVDIFFMAE. To further study this relationship between BERR and reduction in MAE on using *stable* labels for evaluation over *real-time* labels by computing the Pearson correlation coefficient (PCC) between BERR and REVDIFFMAE for in Table 3. As seen from Figure 3, we observe that for YYG, PCC is positive, indicating that YYG’s scores are actually due to larger BERR on labels. We also see significant differences in PCC for YYG and CMU-TS in over other models.

Table 3: Pearson Correlation Coefficient (PCC) between BERR and REVDIFFMAE using stable labels over real-time labels

Model	PCC
ENSEMBLE	-0.327
GT-DC	-0.322
YYG	0.110
UMASS-MB	-0.291
CMU-TS	-0.468

C Hyperparameters

In this section we describe in detail hyperparameters related to data preprocessing and B2F architecture.

C.1 Data Pre-processing

Missing real-time data Sometimes there is a delay in receiving signals for current week. In this case we use values from most revised version of last observation week for real-time forecasting.

Missing revisions Once we start observing a signal $d_t^{(t)}$ from week t till t_f , there are weeks t' in between where the revised value of this signals is not available or value received is zero. This gives rise to *Spike* behaviour (Figure 2). Before training we replace this value with previous value of BSEQ.

Termination of revisions We observed that for some digital signals, revisions stops a few months in future. This could be due to termination of data correction for that signal for older observation weeks. In such cases, we assume that signals are stabilized and use the last available revised values to fill the following values of BSEQ.

Scaling signal values Since each signal, that is received have very different range of values, we rescale each individual signals with mean 0. and standard deviation 1.0. Note that since B2F is trained separately for each each week, we normalize the data for each week before training.

C.2 Architecture

BSEQENC The dimension size of all latent encodings $h_{i,t'}^{(t')}$ and $v_{i,t'}^{(t')}$ is set to 50. Each *GConv* is a single layer of graph convolutional neural network with weight matrix of size $\mathbb{R}^{50 \times 50}$.

MODELPREDENC For *GRU_{ME}* We use a GRU of single hidden layer with output size 50.

REFINER the feed-forward network *FFN_{RF}* is a 2 layer network with hidden layers of size 60 and 30 followed by final layer outputting 1 dimensional scalar.

Training hyperparameters We used learning rate of 10^{-3} for pre-training and 5×10^{-4} for fine-tuning. Pretraining task usually around takes 2000 epoch to train with first 1000 epochs using teacher

forcing and each of rest of the epoch using teacher forcing with probability 0.5. Fine-tuning takes between 500 to 1000 epoch depending on the model, region and week of forecast.

Overall, we found that most hyperparameters are not sensitive. The most sensitive ones mentioned in main paper are $c \in \{2, 3, 4, 5\}$ that controls sparsity of graph G_t and $l = 5$ that controls how many steps we auto-regress using BSEQENC to derive latent encodings for BSEQ during inference.

D Results for MAE and MAPE

We show the average % improvements of all baselines and B2F in Table 4 including for $k = 1$ week ahead forecasts (We show for $k = 2, 3, 4$ in main paper Table 2 as well). B2F clearly outperforms all baselines and provides similar improvements for COVID-19 Forecast Hub models for $k = 1$ week ahead forecasts as described in Section 4 for other values of k .

Table 4: % improvement in MAE and MAPE scores averaged over all regions from May 2020 to Dec 2020

Cand. Model	Refining Model	K=1		k=2		k=3		k=4	
		MAE	MAPE	MAE	MAPE	MAE	MAPE	MAE	MAPE
Ensemble	FFNREG	-0.21	-0.45	-0.35	-0.12	0.48	-0.29	0.81	0.36
	PREDRNN	-1.67	-0.61	-2.23	-1.57	-1.51	-3.78	-1.13	-2.36
	BSEQREG2	0.15	0.19	-1.45	-2.73	-1.74	-3.21	-5.2	-4.78
	BSEQREG	2.1	0.29	1.42	0.37	0.37	0.22	0.72	0.28
	B2F	6.22	6.13	5.18	5.47	3.64	3.9	3.61	6.3
GT-DC	FFNREG	-1.92	-1.45	-2.42	-1.51	-2.04	-6.07	-1.86	-0.49
	PREDRNN	-3.9	-4.44	-3.02	-3.41	-2.62	-3.95	-2.81	-3.26
	BSEQREG2	0.51	0.46	2.24	3.51	2.31	2.42	1.6	0.57
	BSEQREG	2.92	2.5	2.13	3.84	3.6	3.55	1.42	2.27
	B2F	10.44	12.37	12.68	12.59	11.42	10.67	9.64	8.97
YYG	FFNREG	-3.45	-1.53	-2.08	-1.34	-4.62	-3.89	-1.37	-3.06
	PREDRNN	-1.47	-0.92	-3.84	-6.99	-5.57	-4.16	-9.29	-5.81
	BSEQREG2	-1.39	-0.59	-1.25	-0.7	-2.57	-3.72	-6.65	-5.45
	BSEQREG	-1.98	-1.92	-1.78	-2.26	-1.99	-1.53	-0.61	-0.43
	B2F	10.64	7.74	8.84	5.98	7.04	7.64	6.8	5.27
Umass-MB	FFNREG	-2.37	-2.03	-3.25	-5.74	-2.16	-3.17	-1.44	-4.84
	PREDRNN	-3.52	-4.61	-8.2	-7.54	-5.19	-7.82	-5.99	-7.43
	BSEQREG2	-1.01	-0.92	-2.16	-1.88	-2.13	-0.67	-2.29	-2.31
	BSEQREG	0.92	0.78	1.58	0.86	-1.26	0.45	0.06	0.03
	B2F	4.44	5.31	5.21	4.92	3.25	4.74	3.94	3.49
CMU-TS	FFNREG	-2.22	-4.17	-5.24	-4.93	-2.87	-1.95	-3.19	-6.7
	PREDRNN	-6.59	-4.11	-8.17	-8.21	-3.32	-6.3	-3.75	-9.1
	BSEQREG2	0.46	0.71	-0.67	-0.57	-0.73	-0.19	-0.38	-0.12
	BSEQREG	1.76	2.34	1.46	1.05	2.74	2.47	2.11	2.84
	B2F	7.54	8.22	8.75	10.48	5.84	7.62	6.93	6.28